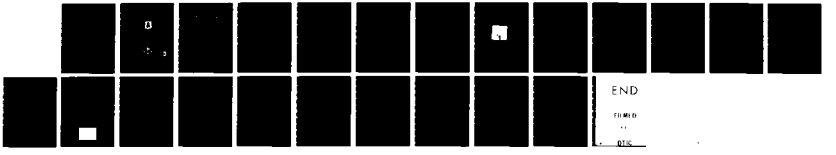

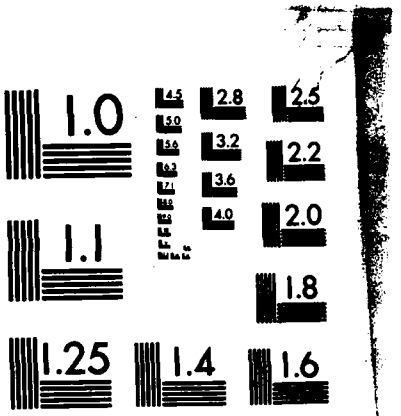

FTD-ID(RS)T-1067-83

# FOREIGN TECHNOLOGY DIVISION

TRANSACTIONS OF THE CHINESE SOLAR ENERGY SOCIETY

(Selected Articles)



Approved for public release;
distribution unlimited.

# EDITED TRANSLATION

FTD-ID(RS)T-1067-83 4 August 1983

MICROFICHE NR: FTD-83-C-000960

TRANSACTIONS OF THE CHINESE SOLAR ENERGY SOCIETY
(Selected Articles)

English pages: 16

Source: Acta Energiae Solaris Sinica, Vol. 3,
Nr. 4, 1982, pp. 449-454; 457-459

Country of origin: China
Translated by: SCITRAN
F33657-81-D-0263
Requester: FTD/TQTD






PREPARED BY:

TRANSLATION DIVISION
FOREIGN TECHNOLOGY DIVISION
WP-AFB, OHIO.

Table of Contents

GRAPHICS DISCLAIMER

All figures, graphics, tables, equations, etc. merged into this translation were extracted from the best quality copy available.

# The Ni/a-Si Schottky Barrier Solar Cell

Sun Zhonglin, Xiong Shaozhen, Wang Zongpan, and Wenyuau
(Nankai University)

## INTRODUCTION

/449

In the three basic types of non-crystalline silicon cells, the development of the M/a-Si Schottky Barrier structure was the earliest. For a while, it was the leader. However, because of the limitation imposed on the open circuit voltage by the work function of the metal, as well as the presence of a stability problem, it does not have sufficient competitive power. Specifically in reference to problems, a wide range of studies have already begun[1-6].

We found that the instability mainly comes from the deterioration of the M/a-Si Schottky structure. This deterioration process not only is affected by the external environment, but also is caused by a solid-solid reaction at the interface. Hence, this deterioration is closely related to the metal. We chose Ni metal as the Schottky barrier metal not only because of its low cost, but also for its stability. Experimental results showed that a Ni/a-Si Schottky battery cell without any protection was not found to have any obvious deterioration after being stored in the atmospheric environment for 20 months statically. The dynamic test for several months also yielded satisfactory results. In addition, corresponding analysis and exploration was also carried out with respect to enlarging the cell area and to practical applications.

## EXPERIMENTAL RESULTS

### 1. Structure and Fabrication of the Cell

Figure 1 is the schematic diagram of the structure of a Schottky barrier Ni/a-Si cell, in which the requirement of the surface is cleanliness of the stainless steel substrate; it is relatively high. The thickness of the $n^+$-a-Si layer deposited on the substrate by the glow discharge of $SiH_4$ + $PH_3$ (2%) is

about 300Å. The resistivity $\rho \simeq 10^2$ Ωcm and $E_c - E_f \simeq 0.2$eV. The undoped a-Si layer thickness is about 5000Å. Furthermore, the growth condition was controlled so that $\rho \simeq 10^7$-$10^{10}$ Ωam, $\gamma = \sigma_p/\sigma_d \simeq 10^2$-$10^4$. In these ranges, cells can be fabricated. The transmissivity of the vapor deposited metallic Ni layer, which was done through heated tungsten wire and masking, is approximately 30%. The surface resistivity is around 40Ω/□. Subsequently, the fabrication of the Ni/Al grid was completed. Finally, vacuum deposition was used to prepare anti-reflecting film of SiO (n values close to 1.9) at around 800Å.

Figure 1. Schematic Diagram of the Structure of a Ni/a-Si Cell.

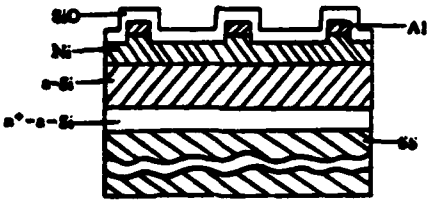


2. Parameters and Characteristics of the Cell.

Among the over one hundred cells already fabricated ($S = 1.3\text{cm}^2$), the conversion efficiency of more than half of them exceeds 1%. Table 1 lists a series of typical parameters. The light source used in the experiment is a Xenon lamp. Furthermore, its intensity was calibrated with a single crystal standard photo cell provided by Tianjing Electrical Power Source Research Institute. The light intensity used in the calculation of the conversion efficiency is AMI (100 mW/cm$^2$).

Table 1. /450

| 1 编号 | 2 参数 $V_{oc}$ (mV) | $I_{sc}$ (mA) | $FF$ | $S$ (cm²) | $\eta$ (%) | 3 减反膜 |
|---|---|---|---|---|---|---|
| 1 | 460 | 8.2 | 0.41 | 1.3 | 1.2 | 4 无 |
| 2 | 440 | 10 | 0.42 | 1.3 | 1.42 | 5 无 |
| 3 | 440 | 6.3 | 0.42 | 1.3 | 0.9 | 6 有 |
| 4 | 400 | 6 | 0.49 | 1.3 | 0.9 | 7 有 |
| 5 | 440 | 13.2 | 0.44 | 2.5 | 1.0 | 8 有 |
| 6 | 420 | 32 | 0.38 | 8.0 | 0.53 | 9 无 |

(Table 1 - Key next page)

1) Number; 2) Parameters; 3) Anti-reflective film; 4) Without 5) Without; 6) With; 7) With; 8) With; 9) Without.

Due to the fact that the light source could not shine uniformly on the 9.0 $cm^2$ cell at AMI light intensity, it is estimated that the short circuit current loss is approximately 30-40%. Figure 2 is the photograph of a real cell, in which the dimensions of a single cell are 2 cm x 4.5 cm.

Figure 3 shows the characteristic output curve of a cell (No. 2).

Figure 2. Photograph of the Actual 9.0 $cm^2$ cell.

Figure 3. Characteristic Output Curve of a Cell (No. 2). FF ~ 0.42, y ~ 1.42%, AMI, 100 $mW/cm^2$.

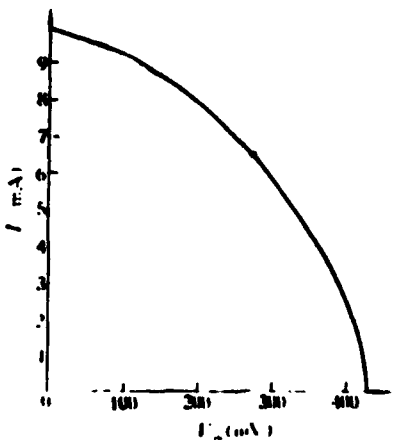

Figure 4 is the spectral responses of $I_{sc}$ and $V_{oc}$ of a cell (No. 3). It is obvious that the wavelength of the maximum of the response curve is fairly close to the maximum value of the solar spectrum. The response curve declines on the long wavelength side, which may be attributed to the fact that the absorption coefficient of the undoped a-Si material decreases with increasing wavelength. The decline on the shorter wavelength side of the peak value may be because of the strong absorption in the a-Si surface layer causing the increase in series resistance. This can be seen from the transmissivity curve of a-Si in Figure 5 (in the 4000Å - 5000Å range, the variation of transmissivity with film thickness is very fast). Of course, the spectral lines in Figure 4 correspond to light of equal energy. Therefore, with decreasing wavelength, the number of photons will also decrease. This should also have an effect on the decline of the spectral lines. We also measured the transmissivity spectrum of the metallic Ni thin film (the dotted line in Figure 5). It increases slightly with decreasing wavelength. However, according to the ion milling Auger spectral analysis of the cell, one knows that for a stabilized cell, there is no pure Ni layer on the top surface of a-Si; instead it is replaced by a silicon compound. Therefore, the light absorption characteristic here is also affected by the Ni silicon compound, which may be completely different from the absorption spectrum of the pure Ni layer. The measurement was made by using a halide tungsten filament lamp as the light source. It was performed on a WDF-1 monochromator.

Figure 4. The $I_{sc}$ and $V_{oc}$ Spectral Responses of the Cell (No. 3). /451

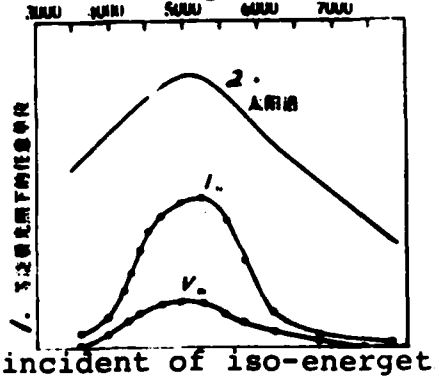


1) Arbitrary unit under the incident of iso-energetic light.
2) Solar spectrum.

Figure 5. Transmissivity Curves of a-Si and Ni Thin Film.

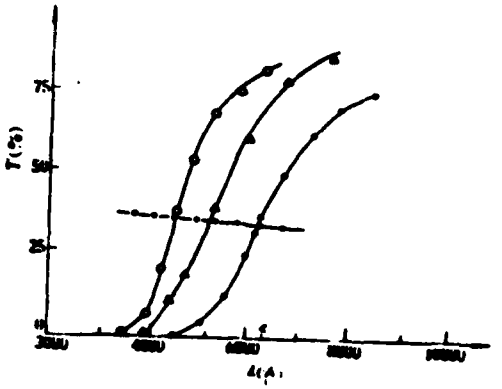

1) Thin Ni layer.

Figure 6. Auger Spectrum of Ni/a-Si

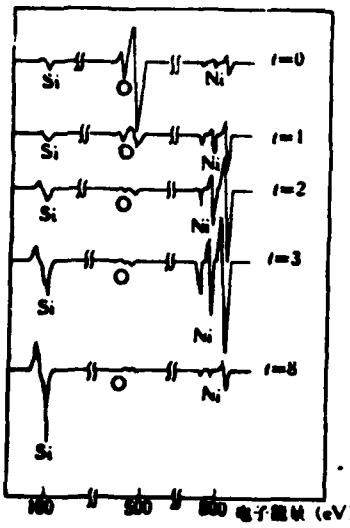


1) Electron energy (eV).

DISCUSSION

1. Stability is a common problem of Schottky barrier non-crystalline silicon cells. In this regard, we have given our special attention. Figure 6 gives the stripping Auger spectra of the Ni/a-Si Schottky junction after a static storage of 14 months (atmosphere and room temperature). One can envision that there was a layer of metallic Ni on the a-Si surface when

the cell was just fabricated. However, because there is a solid-solid mutual diffusion process between the Ni layer and a-Si, the pure Ni layer will eventually disappear when it finally becomes stable. Since we are mainly concerned with the long term stability of the junction, therefore we did not perform any individual study on the disappearance process of the metal film. From the variation of the characteristic peak amplitude with stripping thickness for each element in the spectra, one can see that there is no more pure Ni layer present on the surface of the final cell.

In the study of metal silicides one knows that only a few elements, approximately over ten, can form compounds with silicon, and Ni is one of them. Its formation energy is relatively low. For example, the Ni-Si phase can be formed at room temperature ($27^{o}C$). In addition, from the ESCA analysis of the sample, one can see that the Ni in the layer has already shifted toward the high energy direction from its pure metallic characteristic peak (852.5eV). This reflects that the Ni in the layer no longer exists independently. Instead, it may be present in the a-Si network in the form of a certain bond. This bond limits the future diffusion of Ni. Consequently, it is stable. As for what type of Ni silicide is formed, it still remains to be compared and verified against the characteristic spectra of standard specimens of Ni silicides. Because the metal silicide produced has metallic characteristics, therefore, it is possible to treat Ni silicide as a metal layer. At this time, the metal-semiconductor contact interface is situated at the Ni silicide and a-Si interface. Obviously, it has already penetrated into a certain depth in the bulk. In addition to the fact that Ni silicides are stable, the junction surface deeply penetrated in the bulk also prevented the effect of external environment on the junction characteristics. The two aforementioned factors may be the key to the stability of solar cells fabricated with the Ni/a-Si Schottky barrier. /452

In order to observe the stability under the working condition of the cell, i.e. the photo-deterioration effect of the a-Si material and the electrical shift effect of the barrier metal, we placed the cells in the atmospheric environment to

measure the variation of the output characteristics with irradiation time under a relatively large current output condition (5 $mA/cm^2$) with indoor sunlight. To date, records have been kept for over half a year. No deterioration has been found yet.

2. Using SiO as an anti-flection film has some problems for a Ni/a-Si Schottky barrier solar cell. First, SiO can easily peel off from the Ni layer (under similar environments, light irradiation can alleviate, or even avoid such effect). In addition, in the SiO vapor coating process, the cells can be easily damaged. The reason is still not clear at the present moment.

3. As far as the Ni/a-Si cells we have fabricated are concerned, in order to further improve the efficiency, the emphasis must be placed on increasing the short circuit current and the filling factor. The quality of the filling factor is not only related to the series resistance and the parallel current resistance, but also is affected by the quality of the diode. We chose the No. 3 cell in Table 1 as a real example in our analysis (its filling factor is relatively low). Figure 7 shows the I-V curve of the cell in the dark as well as under light (AMI). For the convenience in comparison, the short circuit current is artificially compensated from the curve under light along the current axis so that it coincides with the dark curve at the origin. From the "light biased" zone in the positive direction of the curve, we found the quality factor n. When the effects of n and $R_s$ on the characteristic curves are simultaneously taken into account, the current-voltage equation can be expressed as

$$J = J_0\left[\exp\left(\frac{V - IR_s}{nkT}\right) - 1\right]$$

in which the value of n can be found through the $\ln J$-$(V-IR_s)$ curve. V is the photon bias plus external positive bias. The $R'_s$ under light and the $R''_s$ in the dark can be obtained either directly or by extrapolation from Figure 8. The measured results are $n_{dark} \sim 2.0$, $n_{light} \sim 1.0$. This result shows that the filling factor is primarily affected by the series resistance in the light

if there are not other influencing factors. Under the light, the value of n approaches the ideal value[7]. That this can be comprehended as the recombination in the barrier zone under light is not apparent. The injection of light (large injection) may cause changes in the barrier zone gap filling. Consequently, the entire recombination process is changed[8]. Apparently, $R_s$ will affect the filling factor under such conditions.

Further analysis of the reverse direction portion of the I-V curve found that despite the reverse,current in the dark is saturated, but it is still not saturated at -0.5V in the light. If this is not caused by a current multiplying effect due to light injection, then this phenomenon can be considered as the result of the expansion of the barrier zone toward the residual neutral zone due to the reverse voltage. This point is also reflected, to a certain extent, by Figures 8 and 9. The effective

Figure 7. I-V Curves of No. 3 Cell in the Dark and Under Light (AMI, 100 mW/cm$^2$), Dark (zero).

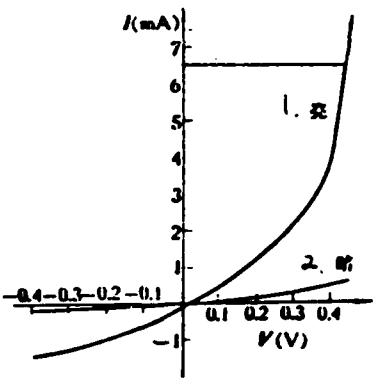


1) Light; 2) Dark.

Figure 8. Correlation Between Effective Internal Resistance of No. 3 Cell and Light Intensity.

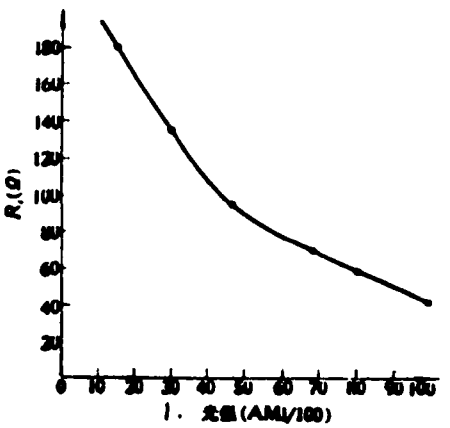


1) Light intensity (AMI/100).

internal resistance in Figure 8 is estimated according to the value of $R_L$ when $V_L = \frac{1}{2}V_{OC}$. Obviously, the $R_s$ obtained by this estimation method is realized to be a function of voltage. Figure 9 happens to prove that the filling curve varies apparently with light intensity. The slope at $\frac{1}{2}V_{OC}$ indeed became smaller with decreasing light intensity. In summary of the above dicussion, to improve the filling factor, the "positive photo-bias" should basically not affect the collection of the photo-current. In other words, the retreat in the field strength in the barrier region should be sufficiently high so that the modulation of the "positive photo-bias" with respect to the barrier width is reduced to a minimum. The fact that it is not saturated in the reverse direction under the light may also be due to the continuous expansion of the strong field region (near the interface) so that the correlation between formation and recombination is reduced[10,11]. This aspect still remains to be analyzed further. In addition to the aforementioned effective internal resistance, the external circuit of the cell also includes the following real series resistance: /453

(a) the resistance between the end of the Ni/Al grid and the point where voltage is obtained, usually less than 4Ω.

(b) the transverse resistance of the barrier metal film. Its calculated value is approximately 4Ω. However, in an actual cell one must consider that Ni silicides have a higher resistance value than that of pure Ni.

(c) the contact resistance between the $N^+$-a-Si and the stainless steel substrate very often becomes a non-ohmic contact type due to the difference in the density of states at the interface[12]. By introducing a Ti thin film as a transition metal layer, it is possible to decrease the resistance of the SS/Ti/$n^+$-a-Si structure to $0.1\Omega/cm^2$.

Figure 9. Relationship Between the Output Characteristics of No. 3 Cell with Light Intensity. (AMI, 100 mW/cm$^2$).

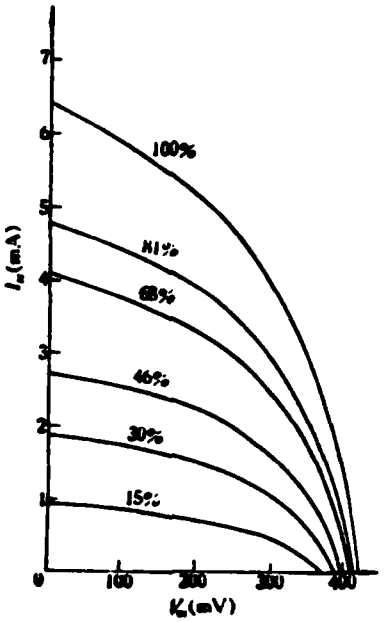


CONCLUSIONS

Despite the fact that the performance of the Ni/a-Si Schottky barrier cell reported in this paper is not very high, as a type of low cost cell, it has its own special features:

Ni is cheaper than those high work function metals such as Pt, Au, Ph. The Ni/a-Si cell is proven to be stable. This cell technology is simple, and it is easy to fabricate large area cells. If the effective internal resistance can be decreased, it is hopeful to have a short circuit current greater than 10 mA/cm$^2$ and a filling factor larger than 0.5. The efficiency will exceed 2%.

Figure 10. Photograph of the Actual Device.

As an attempt, under indoor sunlight and fluorescent lights, /454 we used this cell to supply electricity to electronic clocks and electronic calculators. It was capable of making them function normally.

REFERENCES


1. J.I. B. Wilson, Proc. 13th IEEE Photovoltaic Specialists Conf., (1978), 751.
2. D.E. Carlson, 2nd E.C. Photovoltaic Solar Energy Conf., (1979), 312.
3. C.C. Tsai, to be published in le Journal de physique, (1981).
4. J. Haller, Bull Am. Phys. Soc., 25 (1980), 294.
5. Li Changjian, et al., Acta Energiae Solaris Sinica, Vol. 2, (1981), No. 3., 331.
6. Sun Zhonglin, et al., Acta Energiae Solaris Sinica, Vol. 3., (1982), No. 2., 216.
7. D.E. Carlson, Appl. Phys. Letter, 26, (1976), 671.
8. W.E. Spear, Advances in Physics, 26, (1977), 811.
9. G.A. Swartz, 14th IEEE Photovoltaic Specialists Conf., (1980), 1224.
10. R. Crandall, Appl. Phys. Letter, 36, (1980), 601.
11. D. Adlar, J. Appl. Phys. 51, (1980), 6429.
12. P.K. Dubey, Appl. Phys. Letter, 29, (1976), 435.

# Heterojunction $SnO_2$/n-Si Solar Cells



Jiang Xuesheng, Yin Wenli, and Li Tong
(Beijing Solar Energy Research Institute)

The heterojunction $SnO_2$/n-Si solar cell can practically be considered as a kind of SIS cell, which is a conductive oxide heterojunction solar cell with a semiconductor-insulator-semiconductor structure. It provides the feasibility of fabricating solar cells at low cost. It avoids high temperature technologies and is more suited for polycrystalline and non-crystalline materials. The anti-reflective characteristic of the $SnO_2$ thin film is good. It has better response at short wavelengths. The chemical stability of the $SnO_2$ thin film is good. It is capable of resisting strong acid solutions, which is beneficial to the environmental protection of the device[1]. The $SnO_2$ thin film can be fabricated by using methods such as vacuum evaporation, sputtering, spraying, and chemical vapor deposition. In this work, the most attractive chemical spraying method was adopted.

## I. FABRICATION OF THE SOLAR CELL

The material used to fabricate the cell is single crystal n(100) silicon slice. Its resistivity is 0.5 - 3 ohm · cm. After chemical cleaning, the silicon wafer was placed in an oven (oven temperature 350°C-400°C). It was baked for 20-40 minutes. Afterwards, a mixture of tin tetrachloride and alcohol or ethyl acetate was sprayed on the silicon wafer in a mist form. After 2-4 minutes, a "dark blue" $SnO_2$ thin film was formed, and its thickness is about 700-1000Å. We used a 0.77M tin tetrachloride solution in ethyl acetate as the spraying mixture[2]. The spraying gas source is high purity nitrogen. Its chemical reaction is:

$$SnCl_4 + 2H_2O \rightarrow SnO_2 + 4HCl\uparrow$$

Then, 400-1000Å of titanium and 1-2μ of silver were vacuum deposited as the back contact metal. A metallic covering mask was used in the vacuum deposition of 400-1000Å of titanium and 2-3μ of silver as the electrode grid on the joint. The structure of the solar cell is shown in Figure 1.

Figure 1. The Cell Structure.

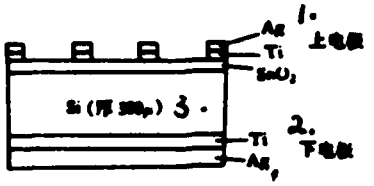

1) Top electrode; 2) Bottom electrode; 3) Si (thickness 300μ).

II. PHOTOELECTRIC CHARACTERISTICS OF THE SOLAR CELL

1. The Volt-Ampere Characteristic

The fabricated $SnO_2$/n-Si solar cell was illuminated under a iodine tungsten lamp at a light intensity of 100 $mW/cm^2$. The volt-ampere characteristic curve as recorded by an x-y recorder is shown in Figure 2. The power conversion efficiency n = 6.5%. The open circuit voltage $V_{oc}$ = 0.51V. The short circuit current density $J_{sc}$ = 24.5 $mA/cm^2$. The filling factor FF = 0.52. The area of the cell is 10 $cm^2$. After subtracting the area of the grids, the cell efficiency is 7.2%.

Figure 2. The I-V Characteristic Curve of the Cell.

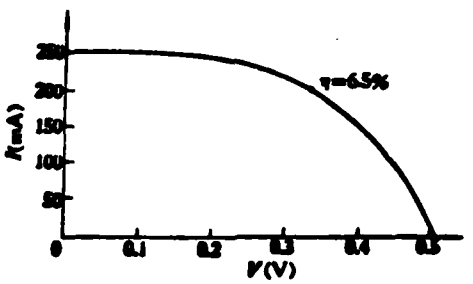


2. The Optical Characteristics of the $SnO_2$ Thin Film.

The geometric thickness of the $SnO_2$ thin film was measured to be 780Å by using an elliptical polarizer. Its index of refraction is ≈ 2. The index of refraction for silicon, however, is ≈ 3.85. According to the matching condition of minimum refractive index in optics, the $SnO_2$ thin film obtained by our spraying has good anti-reflective characteristics. A bromine tungsten lamp flooding reflection integral sphere method was used to measure that the average reflectivity of a silicon wafer without /458

the sprayed $SnO_2$ thin film was 43% in the entire spectral range. After being sprayed with a $SnO_2$ thin film, the average reflectivity was 21%.

3. The Spectral Response

A piece of spectrally standardized n/p type silicon solar cell was selected as the reference. A comparison method was used to measure the relative spectral response of the $SnO_2$/n-Si solar cell. The schematic diagram of the measurement is shown in Figure 3. 10 pieces of filters with different wavelengths were used to measure the spectral current $j_1(\lambda)$ of the n/p type silicon cell and the spectral current $j_2(\lambda)$ of the $SnO_2$/n-Si cell. Let us assume that the spectral response of the n/p type silicon cell is $Q_1(\lambda)$, then the spectral response $Q_2(\lambda)$ for the $SnO_2$/n-Si cell to be measured is

$$Q_2(\lambda)=\left[\frac{j_2(\lambda)}{j_1(\lambda)}\right]\cdot Q_1(\lambda) \qquad \text{(A)}$$

The spectral response curves are shown in Figure 4. Although our measuring apparatus is relatively simple, the quality of the filters is also poor, and the error of measurement is relatively large, yet we can see from the spectral response curves that the spectral response of the $SnO_2$/n-Si solar cell fabricated by us is more or less the same as that of the n/p type silicon solar cell. The short wavelength response was slightly improved.

Figure 3. Schematic Diagram of the Spectral Response Movement.

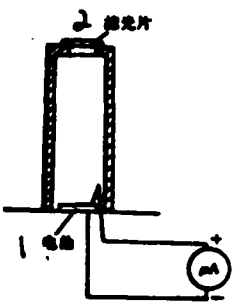

1) Cell; 2) Filter.

Figure 4. Comparison of the Spectral Response Curves of a $SnO_2$/n-Si Cell and a n/p Type Silicon Cell.

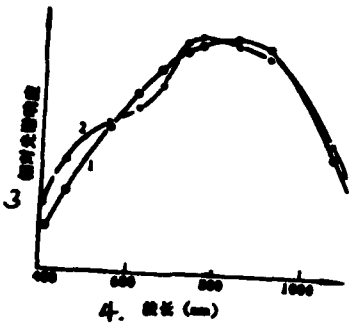

1) n/p type silicon cell; 2) $SnO_2$/n-Si cell; 3) Relative spectral response; 4) Wavelength (nm).

## III. DISCUSSION

The filling factor of the $SnO_2$/n-Si solar cell we fabricated is relatively low, FF = 0.52, and this is the major problem affecting the power output of the solar cell. It was caused by excessive series resistance and junction current. Because the range of work function of $SnO_2$ varies greatly[3], its corresponding barrier light also varies largely. Therefore, in order to improve the p-n junction characteristics of the cell and to reduce the thin layer resistance of the $SnO_2$ film, as long as the spraying technique to form the junction is controlled and the contact resistance on both sides of the cell is improved, the output power will be greatly increased.

The theoretical value of the open circuit voltage of the $SnO_2$/n-Si solar cell we fabricated is approximately 0.6V. However, the actual measured open circuit voltage is $V_{oc}$= 0.51V. Therefore, it is slightly lower. Usually, before forming a $SnO_2$ thin film by spraying, a thin insulating layer of $SiO_2$ is formed on the silicon surface by heating. Its purposes are to improve the diode quality factor and to reduce the saturated dark current to consequently increase the open circuit voltage of the solar cell[4]. Because the thickness of the SiO2 insulating layer strongly affects the open circuit current and the short circuit current, if the $SiO_2$ thickness can be controlled to the optimum (usually it is 10-30Å), then the photovoltaic characteristics of the $SnO_2$/n-Si solar cell will definitely be improved to a certain extent.

Those who participated in this work also include Yao Kexian /459
and Tianxing. Chen Hong, Sun Xiaolu, He Zinian, and Ren Manwen assisted in analysis and measurement. We wish to express our thanks.

This paper was received on January 14, 1982.

REFERENCES

1. E. Saucedo and J.M. Arroyo, 14th IEEE Photovoltaic Specialists Conference, P. 1370-1375, (1980).

2. T. Feng, A.K. Ghosh and C. Fishman, Appl. Phys. Lett., Vol. 35, No. 3, P. 266-268, (1979).

3. T. Feng, C. Fishman and A.K. Ghosh, 13th IEEE Photovoltaic Specialists Conference, P. 519-523, (1978).

4. T. Nagatomo, M. Endo and O. Omoto, Jap. J. Appl. Phys., Vol. 18, No. 6, P. 1103-1109, (1979).

DISTRIBUTION LIST

DISTRIBUTION DIRECT TO RECIPIENT

| ORGANIZATION | MICROFICHE |
|---|---|
| A205 DMAHTC | 1 |
| A210 DMAAC | 1 |
| B344 DIA/RTS-2C | 9 |
| C043 USAMIIA | 1 |
| C500 TRADOC | 1 |
| C509 BALLISTIC RES LAB | 1 |
| C510 R&T LABS/AVRADCOM | 1 |
| C513 ARRADCOM | 1 |
| C535 AVRADCOM/TSARCOM | 1 |
| C539 TRASANA | 1 |
| C591 FSTC | 4 |
| C619 MIA REDSTONE | 1 |
| D008 NISC | 1 |
| E053 HQ USAF/INET | 1 |
| E403 AFSC/INA | 1 |
| E404 AEDC/DOF | 1 |
| E408 AFWL | 1 |
| E410 AD/IND | 1 |
| E429 SD/IND | 1 |
| P005 DOE/ISA/DDI | 1 |
| P050 CIA/OCR/ADD/SD | 2 |
| AFIT/LDE | 1 |
| FTD | |
| CCN | 1 |
| NIA/PHS | 1 |
| NIIS | 2 |
| LLNL/Code L-389 | 1 |
| NASA/NST-44 | 1 |
| NSA/1213/TDL | 2 |

END

FILMED

9-83

DTIC